ANNUAL REVIEWS

Stability of Ice Shelves and Ice Cliffs in a Changing Climate

Jeremy N. Bassis,[1] Anna Crawford,[2,3]
Samuel B. Kachuck,[1] Douglas I. Benn,[4]
Catherine Walker,[5] Joanna Millstein,[6]
Ravindra Duddu,[7] Jan Åström,[8] Helen A. Fricker,[9]
and Adrian Luckman[10]

[1]Department of Climate and Space Sciences and Engineering, University of Michigan, Ann Arbor, Michigan, USA; email: jbassis@umich.edu

[2]Division of Biological and Environmental Sciences, University of Stirling, Stirling, United Kingdom

[3]School of GeoSciences, University of Edinburgh, Edinburgh, United Kingdom

[4]School of Geography and Sustainable Development, University of St Andrews, Fife, United Kingdom

[5]Department of Applied Ocean Physics and Engineering, Woods Hole Oceanographic Institution, Woods Hole, Massachusetts, USA

[6]Department of Geophysics, Colorado School of Mines, Golden, Colorado, USA

[7]Department of Civil and Environmental Engineering and Department of Earth and Environmental Sciences, Vanderbilt University, Nashville, Tennessee, USA

[8]CSC—IT Center for Science Ltd., Esbo, Finland

[9]Scripps Institution of Oceanography, University of California San Diego, La Jolla, California, USA

[10]Department of Geography, Faculty of Science and Engineering, Swansea University, Swansea, United Kingdom

ANNUAL REVIEWS CONNECT

www.annualreviews.org

- Download figures
- Navigate cited references
- Keyword search
- Explore related articles
- Share via email or social media

Keywords

ice sheet, ice shelf, iceberg, calving, sea-level rise, climate

Abstract

The largest uncertainty in future sea-level rise is loss of ice from the Greenland and Antarctic Ice Sheets. Ice shelves, freely floating platforms of ice that fringe the ice sheets, play a crucial role in restraining discharge of grounded ice into the ocean through buttressing. However, since the 1990s, several ice shelves have thinned, retreated, and collapsed. If this pattern continues, it could expose thick cliffs that become structurally unstable and collapse in a process called marine ice cliff instability (MICI). However, the feedbacks between calving, retreat, and other forcings are not well understood. Here we review observed modes of calving from ice shelves and marine-terminating glaciers, and their relation to environmental forces. We show

that the primary driver of calving is long-term internal glaciological stress, but as ice shelves thin they may become more vulnerable to environmental forcing. This vulnerability—and the potential for MICI—comes from a combination of the distribution of preexisting flaws within the ice and regions where the stress is large enough to initiate fracture. Although significant progress has been made modeling these processes, theories must now be tested against a wide range of environmental and glaciological conditions in both modern and paleo conditions.

- Ice shelves, floating platforms of ice fed by ice sheets, shed mass in a near-instantaneous fashion through iceberg calving.
- Most ice shelves exhibit a stable cycle of calving front advance and retreat that is insensitive to small changes in environmental conditions.
- Some ice shelves have retreated or collapsed completely, and in the future this could expose thick cliffs that could become structurally unstable called ice cliff instability.
- The potential for ice shelf and ice cliff instability is controlled by the presence and evolution of flaws or fractures within the ice.

1. INTRODUCTION

Ice sheets are thick masses of ice that accumulate on land through snowfall and then flow toward the ocean, where they form platforms of floating ice called ice shelves. Ice shelves play a crucial role in modulating the dynamics of the grounded ice through their contact with walls and bathymetric highs (pinning points) through a process known as buttressing (Goldberg et al. 2009, Hughes 1977, Hughes et al. 1977, Thomas & MacAyeal 1978, Weertman 1974). Ice shelves are located near sea level and thus are in contact with both the atmosphere and ocean, making them sensitive to climate forcing. Over the past three decades, we have seen thinning and acceleration of the ice shelves that surround the Antarctic Ice Sheet (e.g., Scambos et al. 2004, Paolo et al. 2015, Pritchard et al. 2009), the Greenland Ice Sheet (e.g., Moon & Joughin 2008, Ruckamp et al. 2019), and Arctic ice shelves (Copland et al. 2017, Mueller et al. 2017a, Vincent et al. 2001). For example, the 2002 collapse of the Larsen B Ice Shelf in the Antarctic Peninsula triggered an acceleration of the glaciers that had previously nourished the ice shelf, demonstrating both the speed at which ice shelves can collapse and the importance of ice shelves in buttressing ice sheets (e.g., Scambos et al. 2004).

Marine-based portions of ice sheets, grounded deep beneath sea level, are vulnerable to collapse through a spectrum of instabilities (Hughes et al. 1977, Mercer 1978, Weertman 1974). Marine ice sheet instability is hypothesized to occur when the ice sheet bed slopes downward into the interior of the ice sheet, and weakening or collapse of fringing ice shelves triggers an irreversible cycle of grounding line retreat and increased mass discharge into the ocean (Mercer 1978, Schoof 2012, Weertman 1974). Marine ice cliff instability (MICI) has only recently been proposed (DeConto & Pollard 2016) and is based on the realization that the height of calving cliffs is limited by the strength of ice (Bassis & Walker 2012). If exposed ice at the grounding line cannot support its own weight, it could trigger an instability resulting in an accelerating cycle of cliff collapse and retreat (Bassis & Walker 2012, DeConto & Pollard 2016). Recent research suggests that in portions of the West Antarctic Ice Sheet, such as Thwaites and Pine Island, ice shelf retreat could expose a grounding line thick enough to trigger ice cliff instability (DeConto & Pollard 2016, Scambos et al. 2017, Wise et al. 2017). This potential for a large-scale calving instability drives the range of projections of sea-level rise (Fox-Kemper et al. 2021). However, MICI has yet to be directly

observed and is currently based on theoretical principles (Bassis & Walker 2012, Bassis et al. 2021, Crawford et al. 2021) and paleo inferences (DeConto & Pollard 2016, Edwards et al. 2019, Wise et al. 2017), resulting in the Intergovernmental Panel on Climate Change including a distinct low-confidence scenario for global sea-level rise (Fox-Kemper et al. 2021).

The processes responsible for ice shelf retreat and, ultimately, ice cliff instability are all related to the role of failure, fracture, and calving in ice shelves. Calving, the process where blocks of ice detach from an ice shelf or glacier, has been well recognized in the literature (e.g., Bassis et al. 2007, Larour et al. 2021, Walker et al. 2015). However, the focus of previous studies has been primarily on calving and retreat of grounded glaciers where the bottom of the ice is in contact with the bed (Benn et al. 2007; Nick et al. 2009, 2010; van der Veen 1996; Vieli & Nick 2011). Less attention has been given to the role that calving and failure play in the structural health and stability of ice shelves. This research landscape, however, is rapidly changing with renewed attention to meltwater-driven ice shelf collapse and concern about the potential collapse of Thwaites and Pine Island Glaciers in the Amundsen Sea Embayment (Banwell & MacAyeal 2015; Rack & Rott 2004; Rott et al. 1998; Scambos et al. 2003, 2017).

In this review, we discuss the environmental and glaciological factors that control ice shelf stability, processes that perturb this stability and, finally, what (may) happen in the aftermath of ice sheet retreat, including evidence for ice cliff instability. We center our attention on stable ice shelves, based on the remarkable fact noted by Alley et al. (2023) that most ice shelves have maintained quasi-static calving fronts for centuries or longer. This stability, despite changes in ocean and atmospheric forcing, and even fluctuations in the speed of ice streams feeding ice shelves (Hulbe & Fahnestock 2007), suggests that at least the embayed ice shelves are stable to modest climate perturbations. We then outline observed modes of calving and the forces that drive calving before examining the different methods that are currently used to predict iceberg calving patterns. Finally, we propose new synergies and research directions that incorporate the growing body of available observations and modeling methods into testable hypotheses. These will be crucial for making systematic advances to predict and project what comes next. Because readers may be unfamiliar with some of the terminology used in glaciology, we define key glaciological terms in the **Supplemental Glossary**.

2. ICE SHELVES AND ICE TONGUES ACROSS CLIMATOLOGICAL AND GLACIOLOGICAL REGIMES

Ice shelves exist across a wide range of sizes and environmental conditions, with floating ice shelves currently found in Antarctica, Greenland, and the Arctic (**Figure 1**). For example, the mighty Ross and Filchner-Ronne Ice Shelves are hundreds of kilometers long with sizes comparable to the state of Texas. The largest ice shelves typically form in embayments or behind bedrock protrusions. Many small ice shelves and ice tongues—narrow ice shelves that flow primarily in one direction— simply extend into the ocean with widely varying sizes: The Erebus Ice Tongue typically extends a little over 10 km into the ocean (**Figure 1**), whereas the Drygalski Ice Tongue can extend as much as 100 km.

Greenland has only small and isolated ice tongues remaining, primarily in northern Greenland (**Figure 1b**). Ice shelves in northern Greenland, such as the Petermann and Nioghalvfjerdsbrae Ice Tongues, are embayed and have also retreated recently (Moon & Joughin 2008, Munchow et al. 2016, Ruckamp et al. 2019). Some of the present floating portions of the Greenland Ice Sheet might be remnants of more extensive ice shelves that spread across large swaths of the Arctic Ocean (England 1999, Grosswald & Hughes 2002). There are hints of once-larger ice shelves throughout the Arctic (Jakobsson et al. 2016, Kilfeather et al. 2011, Mercer 1970,
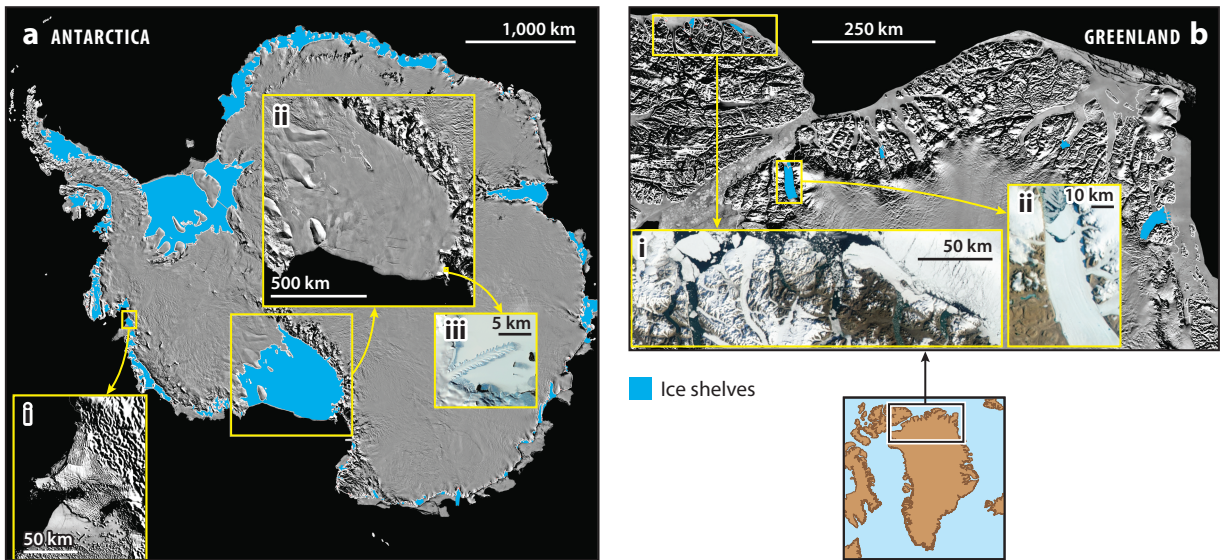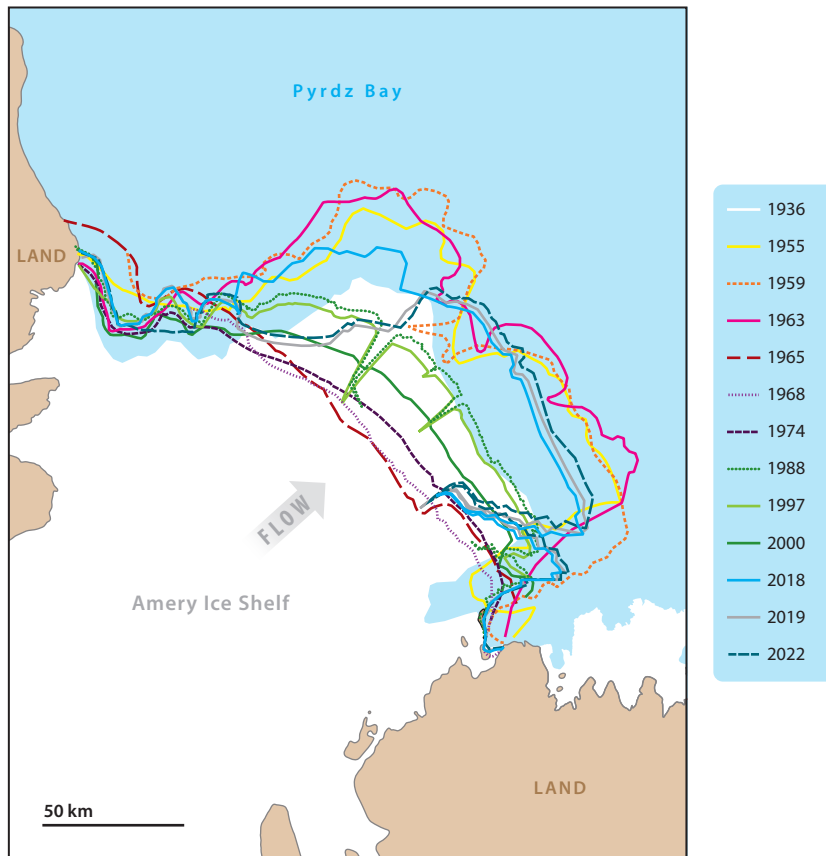
Figure 1

Ice shelves exhibit a variety of shapes and sizes: ice shelves (*shaded blue*) over Moderate Resolution Imaging Spectroradiometer (MODIS) mosaics of (*a*) Antarctica (Haran et al. 2018b) and (*b*) Greenland (Haran et al. 2018a). Insets with different scalebars demonstrate the wide range: (*a,i*) Thwaites Ice Shelf, showing extensive fragmentation of the western ice tongue (MODIS); (*a,ii*) Ross Ice Shelf (MODIS); (*a,iii*) Erebus Ice Tongue [Advanced Spaceborne Thermal Emission and Reflection Radiometer (ASTER), 2001]; (*b,i*) the Ellesmere Island Ice Shelves (Mueller et al. 2017b) after the August 2010 breakup of the Ward Hunt Ice Shelf (NASA Earth Observatory, 2010); and (*b,ii*) Petermann Ice Shelf (Hoyle 2021), showing the tabular iceberg that detached in July 2012 (NASA Earth Observatory, 2012).

Polyak et al. 2001, Vermassen et al. 2020), but there is a paucity of geological evidence to constrain past ice shelf extents. Currently, only a handful of small ice shelves remain in the Arctic, including the vestiges of the once-extensive Ellesmere Ice Shelf (England et al. 2008, 2017; Jeffries 1992, 2017; Mueller et al. 2017a; Vincent & Mueller 2020; Vincent et al. 2001), and in the Severnaya Zemlya and Franz Joseph Land archipelagos (Dowdeswell 2017, Dowdeswell et al. 1994, Williams & Dowdeswell 2001). It is unclear how long these remaining shelves will last as over a dozen ice shelf calving events over the past decades have left the Ellesmere Island Ice Shelf fringe in tatters (Mueller et al. 2017a,b; White et al. 2015).

3. CALVING, FRACTURE, AND STABILITY OF ICE SHELVES AND GLACIERS

Despite the variety of environments, ice shelves and marine-terminating glaciers end in near-vertical cliffs submerged in the ocean. These cliffs are called calving fronts or calving cliffs because fracture ultimately leads to the detachment of icebergs from glaciers and ice shelves. The mechanism responsible for this, the iceberg calving process, can result in a quasi-stable cycle of calving front advance and retreat (e.g., Fricker et al. 2002, Lazzara et al. 2008). However, the very concept of stability is fraught with conflicting definitions and practical difficulties distinguishing stable systems from slowly changing systems (e.g., Glendinning 1994). Our definition of stability is based on an average over time; although the calving front may fluctuate, there are recurring patterns in the size and frequency of events and the calving front fluctuates, but advance and retreat episodes do not breach a minimum extent (Fricker et al. 2002, Lazzara et al. 2008). **Figure 2**, for example,

Figure 2

Advance and retreat of Amery Ice Shelf, East Antarctica, from 1936 to 2022. The Amery Ice Shelf, like most large ice shelves, has multidecadal periods of advance where few icebergs detach. Retreat occurs in a sequence of large tabular calving events that return the calving front to a location closer to the embayment. Figure adapted from Fricker et al. (2002).

illustrates the multidecadal advance and retreat of the Amery Ice Shelf, which recently experienced several large calving events returning the ice shelf from a historically advanced position to close to its historical minimum (Fricker et al. 2002, Walker et al. 2021).

Stable periods of ice shelf advance and retreat can, however, be interrupted by periods of rapid change where the calving front rapidly retreats behind previously documented minimum extents. In Greenland, the floating portion of Sermeq Kujalleq (Jakobshavn Isbræ) thinned and eventually disintegrated starting in the late 1990s, leading to an acceleration of the grounded portion of the ice sheet (Echelmeyer et al. 1991, Holland et al. 2008, Joughin et al. 2004). Observed episodes of rapid retreat correspond to transitions between calving regimes (Alley et al. 2023) and are often accompanied by pronounced changes in the pattern or mode of calving, including size and frequency of icebergs produced (e.g., Walter et al. 2010). Factors controlling both the stability of calving patterns and the underlying iceberg size/frequency distributions provide key insights into processes governing stability (Bassis & Jacobs 2013, Benn et al. 2007, Walter et al. 2010). This process-level understanding is particularly important when extrapolating projections to the future when glaciological and climatological conditions may be different from today.

4. AN INCOMPLETE TAXONOMY OF MARINE CALVING REGIMES

Given the wide variety of calving regimes, in this section, we summarize observations of recent ice shelf and marine glacier behavior, focusing on the characteristics of stable systems (i.e., those that have maintained a consistent minimum frontal position over decades to centuries) and transitions to unstable retreat system states (i.e., those that exhibit episodes of rapid and/or sustained retreat). Our interest, however, is in identifying broad end member patterns in calving styles based on iceberg size and frequency that can ultimately be associated with fracture processes (**Figure 3**). We include marine glacier regimes in our spectrum because retreat or collapse of ice shelves eventually exposes cliffs grounded deep beneath sea level, a prerequisite for MICI. Moreover, evidence from the Arctic, Greenland, and the Antarctic Peninsula suggests that once ice shelves are gone, they rarely re-form under modern climate conditions. Hence, these grounded calving systems may represent the future of today's ice shelves.

## 4.1. Episodic Tabular Iceberg Detachment

Most ice shelves exhibit a pattern of slow advance punctuated by episodic retreat by calving that occurs when one or more rifts—fractures that penetrate the entire ice shelf thickness—isolate and separate an iceberg from the ice shelf (**Figures 2** and **3c**). The timescale between these major calving events is often measured in decades or longer (e.g., Bassis et al. 2007, 2008; De Rydt et al. 2018; Fricker et al. 2002; Joughin & MacAyeal 2005; Lazzara et al. 2008), but these sporadic icebergs can be large, removing decades of accumulated ice shelf mass nearly instantaneously. For example, in May 2021, an iceberg approximately 170 km long and 25 km wide (110 mi by 16 mi) with the dreary name A-76 detached from the Filcher-Ronne Ice Shelf. This tabular calving mode is observed in all regions with floating ice shelves, including Greenland and Ellesmere Island Ice Shelves. The tabular calving style is ultimately controlled by the initiation and propagation of rifts. Rifts, typically initiate upstream along the margins of embayed ice shelves or downstream of local grounding on bathymetric highs (pinning points) or other features that concentrate stress (Benn et al. 2022; De Rydt et al. 2018, 2019; Walker et al. 2013, 2015). Rifts often become stagnant after initiating (Hulbe et al. 2010, Kulessa et al. 2014, Walker et al. 2013), especially when rifts intersect with marine ice–filled suture zones (Borstad et al. 2017, Kulessa et al. 2014).

## 4.2. Explosive Meltwater-Triggered Ice Shelf Disintegration

Although observations indicate that the calving fronts of many ice shelves are stable, the potential for rapid ice shelf collapse (**Figure 3a**) was dramatically illustrated by the explosive meltwater-related disintegration of sections of the Larsen A and B Ice Shelves in the Antarctic Peninsula (MacAyeal et al. 2003, Rack & Rott 2004, Rott et al. 1998, Scambos et al. 2003, Skvarca 1993). Increased tabular calving resulted in the gradual retreat of the ice shelf until, suddenly, in 2002 the Larsen B Ice Shelf explosively disintegrated in fewer than 6 weeks (e.g., Rack & Rott 2004, Scambos et al. 2003). The ice shelf—about the size of Rhode Island—had been stable for thousands of years before disintegrating into a plume of small, needle-shaped icebergs (Alley et al. 2023, Domack et al. 2005, Rack & Rott 2004, Scambos et al. 2003). The disintegration of sections of the Larsen was the culmination of a longer-term retreat of the northernmost Antarctic Peninsula ice shelves coincident with increased atmospheric temperatures across the Antarctic Peninsula (Vaughan & Doake 1996). This style of catastrophic disintegration of ice shelves is linked to the formation of melt ponds on the surface of the shelf that are hypothesized to have triggered extensive hydrofracturing of the ice shelf and, ultimately, the explosive disintegration (Banwell et al. 2014, Banwell & MacAyeal 2015, Banwell et al. 2013, Scambos et al. 2003).
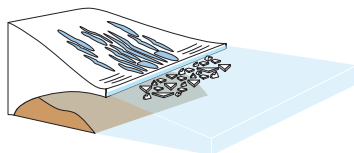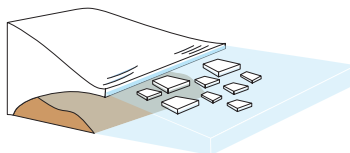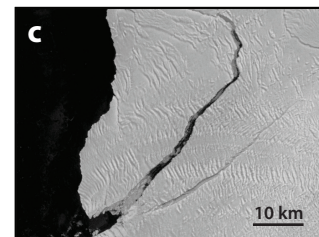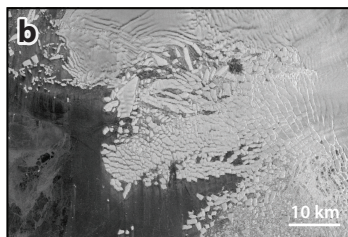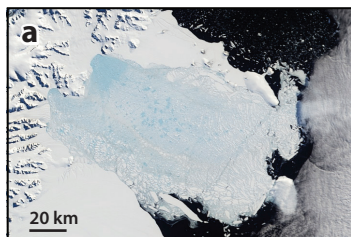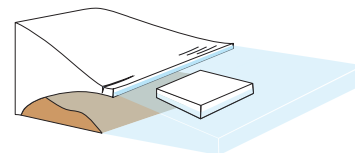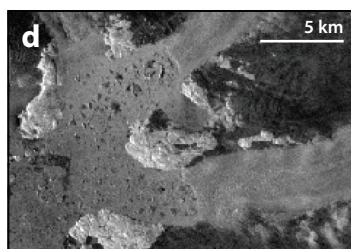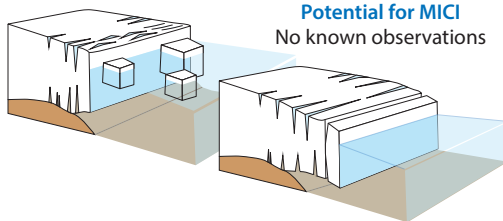
Figure 3

Schematic illustrating the different regimes of calving along with the approximate timescales, with examples from satellite imagery. For floating ice shelves, the fastest mode of calving is explosive disintegration, such as the meltwater-triggered collapse of the Larsen B Ice Shelf (Scambos et al. 2003) shown here in Moderate Resolution Imaging Spectroradiometer (MODIS) imagery (*a*). Ice shelves can also undergo a fragmentation style of calving where kilometer-sized bergs regularly detach, such as Thwaites Glacier (*b*) (Sentinel-1 image). The standard mode of calving from ice shelves is the multidecadal detachment of tabular icebergs, such as Amery Ice Shelf (**Figure 2**) and Brunt Ice Shelf (*c*) (Sentinel-1 image). For grounded marine-terminating glaciers, calving events take place on daily to monthly timescales and remove ice thickness–sized bergs, such as Upernavik Glacier (*d*) (Sentinel-1 image). If the cliff at the calving front exceeds a critical height, it can become structurally unstable, resulting in an unstable cycle of retreat called marine ice cliff instability (MICI), for which we have few observations.

4.3. Fragmentation and Accelerated Rifting

A sequence of calving and rifting events from the Thwaites Glacier in the Amundsen Sea Embayment resulted in the transition of the Thwaites Glacier Western Tongue from a largely intact tongue that shed tabular bergs to a fragmented remnant (**Figure 3b**). The remnants consist of a mixture of kilometer-sized icebergs bound together by a mixture of icebergs, sea ice, and fast ice (Alley et al. 2021, Miles et al. 2020). This style of calving has been previously termed disintegration, but we prefer the term fragmentation. The disarticulation and fragmentation of the Thwaites Ice Tongue followed a string of tabular calving events that resulted in the unpinning of the ice shelf from a bedrock high (Miles et al. 2020). The eastern portion of the Thwaites Glacier Tongue remains intact, but large-scale fractures have propagated across large sections of the ice shelf in a process that is linked to increased compression as the shelf abuts a bathymetric high that serves as a pinning point (Alley et al. 2021, Benn et al. 2022). Evidence for this mode of calving is also found in Pine Island Glacier, where more frequent tabular berg detachment combined with a fragmentation style of calving in margins contribute to ice front retreat (Jeong et al. 2016, Joughin et al. 2021, Liu et al. 2015). The slow fragmentation associated with Thwaites is similarly visible in the Totten Ice Shelf, in East Antarctica, which has also experienced large basal melt rates with a fragmented ice shelf that retreats through relatively smaller iceberg calving events (Liu et al. 2015). Smaller ice shelves fringing the Antarctic Ice Sheet, such as Cook in East Antarctica, have also experienced retreat punctuated by fragmentation (Miles et al. 2018).

4.4. Marine Glacier Calving and Ice Cliff Instability

Marine glacier calving has been reviewed extensively before (e.g., Benn & Astrom 2018, Benn et al. 2007, van der Veen 1996). We focus here on summarizing styles of calving typical of large glaciers that might be exposed in the aftermath of ice shelf retreat or collapse. Typical calving events from marine glaciers take on a variety of patterns, but the icebergs are usually much smaller and more frequent than those that detach from floating ice—on the order of the ice thickness of the glacier with separation on daily to monthly timescales compared to those that detach from floating ice (**Figure 3d**). Some of the thickest Greenland glaciers, such as Sermeq Kujalleq (Jakobshavn Isbræ), have ice cliff heights that may currently approach the threshold necessary to, at least occasionally, trigger ice cliff structural failure (e.g., Parizek et al. 2019). Similarly, the portion of the calving cliff of Crane Glacier in the Antarctic Peninsula that extends above the waterline exceeded 100 m following the collapse of the Larsen B Ice Shelf; it retreated rapidly, thinned, and then readvanced, suggesting that, at least in this case, cliff failure did not lead to catastrophically unstable retreat (Needell & Holschuh 2023).

Evidence to support ice cliff instability from the paleorecord is spotty. DeConto & Pollard (2016) inferred that ice cliff instability was necessary to explain past variations in sea-level rise. However, subsequent work has pointed out that large uncertainties associated with past climate forcing cloud inferences about the relative roles of climate forcing and ice cliff instability in explaining sea-level variations (Edwards et al. 2019). At present, the most direct evidence to support ice cliff instability comes from iceberg scour marks in the Amundsen Sea Embayment with shapes, extents, and depths consistent with rapid, full-thickness calving (Wise et al. 2017). Moreover, it is clear from paleo proxies that grounding lines have retreated much more rapidly in the past than currently observed (e.g., Bart & Kratochvil 2022, Batchelor et al. 2023, Graham et al. 2022), and there are hints in the paleorecord that past ice shelf disintegration events exposed grounded cliffs (e.g., Bart & Kratochvil 2022, Majewski et al. 2018, Wise et al. 2017). Integrating clues from the paleorecord to the mechanical processes that operated in the past or might operate in the future

remains an ongoing challenge, but the emerging evidence clearly highlights the potential for rapid ice shelf change.

5. CONTROLS ON THE STABILITY AND VIABILITY OF ICE SHELVES AND MARINE GLACIERS

Despite the stability of many ice shelves, there is a growing catalog of evidence that both long-term and short-term environmental forcings are increasingly pushing ice shelves outside of their previously quasi-stable regimes. Given the wide variety of calving regimes and potential drivers of calving behavior, we review evidence for (Section 5.1) glaciological and environmental controls on ice shelf evolution, and then (Sections 5.2–5.4) the impact of both shorter- and longer-term forcing on ice shelves.

5.1. Glaciological Controls on Ice Shelf and Glacier Stability

Ice shelves form under a complex assortment of climatologic and glaciologic conditions. Despite the variety of conditions, the dominant mode of calving from ice shelves is the sporadic detachment of tabular bergs resulting in a quasi-stable calving front position. Moreover, given the quasi-stability of the calving front of most ice shelves and decades-long quiescence periods between major calving events, this mode of calving appears to be primarily controlled by the internal glaciological stress within the ice. The geometry of ice shelves clearly exerts a significant control on the long-term stress. The embayment and grounding on bathymetric highs (i.e., pinning points) that confine many ice shelves provide backstress that can offset extensional stresses. The down-glacier limit of such regions defines a compressive arch (Doake et al. 1998). In their prescient paper, Doake et al. (1998) proposed that a compressive arch, consisting of compressive stress trajectories forming a bridge across the ice shelf, constitutes a criterion for ice shelf stability. They hypothesized that retreat of the Larsen B shelf would inevitably follow if the ice front continued to retreat, a reality that was observed four years later with the explosive disintegration of the Larsen B (e.g., Rack & Rott 2004). Unconfined ice tongues, however, lack a compressive arch, yet they still exhibit similar cycles of tabular berg detachment as those that are confined. This suggests that a lack of confinement is not necessarily a prerequisite for instability or collapse. There is also evidence that rift propagation and iceberg calving in ice shelves can, at least under some circumstances, be driven by ocean swell (Aster et al. 2021, Lipovsky 2018, Olinger et al. 2019), tsunamis (Brunt et al. 2011, Walker et al. 2015), and atmospheric rivers (Wille et al. 2022).

5.2. Atmospheric Forcing

Early theories connected the demise of Antarctic Peninsula ice shelves with the mean annual 2 m −5°C atmospheric isotherm, suggesting that ice shelves in regions with warmer temperatures were not viable (Vaughan & Doake 1996). This limit was based on the observation that no ice shelves were present surrounding the Antarctic Ice Sheet where the −5°C annual isotherm was exceeded. In the aftermath of the explosive disintegration of the Larsen B Ice Shelf, Scambos et al. (2003) suggested that viability was instead connected to the −1.5°C summer isotherm associated with significant surface meltwater production. Considering only the summer temperatures shifts a larger set of ice shelves into the danger zone of viability because many ice shelves, such as the Amery Ice Shelf, already experience significant summer melt despite currently frigid winters (Phillips 1998, Scambos et al. 2003, Spergel et al. 2021). Studies have also pointed to sustained exposure to atmospheric rivers as a risk factor contributing to calving and disintegration of Antarctic Peninsula

ice shelves (e.g., Wille et al. 2022). Atmospheric rivers could contribute to ice shelf vulnerability because of the tendency to increase surface melt, but atmospheric rivers are also associated with decreased sea ice extent, increased sea surface slope, and high winds (Francis et al. 2021, 2022; Wille et al. 2022). However, a more nuanced understanding of the role of melt is emerging. Firn densification plays a key role in creating the conditions where melt ponds can form (van Wessem et al. 2023). Glaciological stress regime limits where hydrofracture is likely (Lai et al. 2020), and efficient drainage of meltwater off the ice shelf through supraglacial river formation can prevent melt ponds from forming (Bell et al. 2017, Dow et al. 2018, Kingslake et al. 2017). All these factors mitigate the vulnerability of ice shelves to surface melt.

5.3. Ocean Forcing

Observations show that for many ice shelves, evolution is more tightly controlled by ocean forcing than by surface melt, and this is especially true for the Amundsen Sea Embayment ice shelves (Alley et al. 2021, Christianson et al. 2016, Davis et al. 2018, Milillo et al. 2019). Recent studies have started to link increased basal melt with enhanced calving (Liu et al. 2015), but the physical mechanisms that control this relationship remain elusive. Observational and theoretical studies show that basal melting can excavate subshelf channels (e.g., Alley et al. 2016, Dutrieux et al. 2013, Jenkins 1991), and increased melt is associated with roughening of the ice shelf (Watkins et al. 2021). Melt channels, in turn, alter the stress distribution within the ice, promoting fracture of the ice (e.g., Dow et al. 2018, Vaughan et al. 2012). Recent studies also illustrate the potential for bottom melting to excavate basal crevasses (Schmidt et al. 2023), a process hypothesized to be related to ice shelf failure and stability (Bassis & Ma 2015). Ocean melt also erodes the ice thickness, reducing contact with pinning points; triggers acceleration of grounded discharge; and promotes shear margin weakening (e.g., Lhermitte et al. 2020). It is clear that in regions such as Pine Island and Thwaites Glaciers, changes in calving patterns have been linked to ocean forcing, but linking ocean forcing to ice shelf retreat and demise remains an active area of research.

5.4. Sea Ice and Landfast Ice

Sea ice, landfast ice (sea ice that is attached or fastened to the land), and the mixture of icebergs and sea ice that clogs fjords have all been hypothesized to play a role in stabilizing ice shelves. Sea ice provides a buffer to ice shelves by dampening the ocean wave energy linked to ice shelf flexure, fracture, and calving (Bromirski et al. 2010, Holdsworth & Glynn 1978, Massom et al. 2018). The disintegration of the Wilkins and Larsen A and B Ice Shelves was hypothesized to be preconditioned by strain at the outer-shelf margins, imparted through ocean swell–induced flexure following reduction in adjacent sea ice (Massom et al. 2018). Crucially low sea ice concentrations have been associated with major calving events along the Antarctic Peninsula (Massom et al. 2018), North Greenland (Reeh et al. 2001), and East Antarctica (Miles et al. 2017). Open-water conditions adjacent to the northwest coast of Ellesmere Island were tied to the majority of ice shelf calving events that occurred between 1997 and 2011 in this region (Copland et al. 2017). By contrast, thick multiyear landfast sea ice might provide mechanical stability in addition to damping ocean swell if the thickness is comparable to the ice shelf thickness. Reduction of multiyear ice can potentially lead to calving and retreat, as observed with the Thwaites Ice Tongue (Miles et al. 2020), and has also been linked to the mechanical stabilization of ice shelves and ice tongues, including the Mertz Ice Tongue, Wilkins Ice Shelf, and Parker Ice Tongue (Gomez-Fell et al. 2022; Massom et al. 2010, 2015; Massom et al. 2018).

6. MODELING FRACTURE, FAILURE, CALVING, AND ICE SHELF STABILITY

The variety and variability of forcings and controlling responses at the calving front present stark challenges for the modeling community in simulating the iceberg calving process. Models need not only reproduce the modes of calving and quasi-stable positions of calving fronts but also explain how the array of climate forcings interacts to destabilize the calving front. Below we summarize the key approaches and organize these approaches roughly by the amount of complexity associated with the method.

6.1. Calving Laws

The highest level of simplification involves formulating so-called calving laws. Although individual calving events are stochastic and remove ice in a near-instantaneous fashion, as shown by Bassis (2011), it is possible to define long-term averages over many calving events. Denoting the vertically averaged calving front position by $L(x, y, t)$, the normal to the calving front by $\vec{n}$, and the component of the velocity normal to the calving front $v_t = \vec{v} \cdot \vec{n}$, we can define a relationship of the form

$$\frac{dL}{dt} = v_t - v_c,$$

1.

where v_c denotes the expected value of length lost due to discrete calving events. Calving laws then either seek to formulate a rate of calving by averaging over many calving events,

$$v_c = f(p_1, p_2, \ldots p_N, t),$$

2.

or determine the average position of the calving front,

$$L = g(p_1, p_2, \ldots p_N, t).$$

3.

Here f and g are functions, and p_i are parameters that determine the calving rate or calving front position. Equation 1 is sometimes written with an additional term that represents frontal melting. However, because Ma & Bassis (2019) showed that frontal melt can promote or suppress calving, we treat the frontal melting as a parameter that affects calving rate v_c. In theory, we should be able to derive a relationship between the two functions f and g from the underlying probability distributions for calving events (Bassis 2011), but this is difficult and most calving laws remain semiheuristic. Currently there is a zoo of calving laws and a growing catalog of unruly glaciers that defy the expectation established by these so-called laws. Given our interest in ice shelves and the transition from floating to grounded cliffs in the aftermath of ice shelf demise, we review some of the more common forms of calving laws that are relevant to floating extensions of ice.

6.1.1. Fixed calving front position.
The simplest and most common calving law used assumes that the calving rate always balances the velocity at the calving front (e.g., Hoffman et al. 2018, Lipscomb et al. 2019). This calving law is easily implemented by holding the ice domain constant but has no physical basis, and the only reason this particular calving law is usable is because the calving fronts of many ice shelves have remained relatively unchanged over the past few centuries. The problem is that these laws are incapable of resolving accelerated rifting, fragmentation, or meltwater-triggered disintegration and should only be used cautiously when applied to simulations of past or future changes.

6.1.2. Minimum ice thickness calving.
Minimum thickness calving laws specify the calving position based on where the ice thickness thins to less than a critical threshold (e.g., Albrecht

et al. 2011). These laws are convenient because they are easy to implement in numerical models and avoid the embarrassment of simulations that allow ice shelves and tongues to protrude far beyond their embayment. This type of calving law, however, does not apply to grounded ice and, even for floating ice, the variety of ice thicknesses observed near the calving fronts of ice shelves is especially stark when we also consider Greenland and Arctic Ice Shelves.

6.1.3. Strain rate–based calving laws. An alternative calving law assumes that the rate at which ice shelves spread controls the calving rate. Alley et al. (2008) showed that the calving rate for a host of ice shelves near steady state was proportional to the strain rate parallel to the calving front. Hindmarsh (2012) later showed that this relationship describes the velocity of embayed ice shelves and may simply emerge as a consequence of the embayed ice shelf geometry. Levermann et al. (2012) proposed an alternative strain rate–based calving law that takes the form $v_c = K\dot{\varepsilon}_\parallel \dot{\varepsilon}_\perp$, where $\dot{\varepsilon}_\parallel$ denotes the positive component of strain rate parallel to the calving front and $\dot{\varepsilon}_\perp$ denotes the positive component of strain rate transverse to the calving front with K a tuning parameter. This eigencalving law has been used to predict the large-scale positions of calving fronts and is especially useful for embayed ice shelves because the transverse spreading rate $\varepsilon_\perp$ is usually small or negative until ice shelves extend beyond their embayment (Albrecht & Levermann 2012, 2014). However, the tuning parameter K varies significantly between ice shelves and glaciers; thus, it is difficult to judge how reliably this law can be extrapolated to new conditions.

6.1.4. Stress-based calving: the von Mises calving law. The von Mises calving law takes a stress-based approach and sets $v_c = v_t \frac{\sigma_{vm}}{\sigma_{max}}$, where σ_{vm} denotes the positive contributions to the effective or von Mises stress at the calving front and σ_{max} denotes a glacier-dependent parameter (Morlighem et al. 2016). This calving law can be tuned to reproduce the calving front behaviors of many glaciers and ice shelves (Campbell et al. 2017, Choi et al. 2018, Morlighem et al. 2016, Yu et al. 2019). However, like the eigencalving law, σ_{max} varies significantly between glaciers, and thus it is difficult to judge how reliably this law can be extrapolated to new conditions. Alternative stress-based calving laws have been widely used to predict the depth of crevasses in glaciers, but this requires an understanding of fracture mechanics, which we introduce next.

6.2. Fracture Mechanics, Crevasse Initiation, and Crevasse Propagation

Iceberg calving is ultimately caused by fractures that isolate an iceberg. Hence, a step up in complexity seeks to understand the factors that control fracture initiation and propagation. One advantage of considering fracture mechanics is that it is possible to include the effect of meltwater filling crevasses to represent hydrofracture and, potentially, explosive ice shelf disintegration of ice shelves. A key to understanding the fracture mechanics literature is that we distinguish between the orientation of loading relative to the fracture orientation. This decomposition results in the classification of loading as mode I (opening mode), mode II (sliding or in-plane shear), and mode III (tearing or out-of-plane shear) (e.g., Broberg 1999, Lawn 1993). Mode I, tensile or opening mode, has received the most attention because of its clear relationship to rifting and crevassing. However, it is mixed mode I and mode II failure that is associated with marine ice cliff failure. Previous studies have extensively reviewed the various approaches used in the glaciological literature to treat fracture of ice (e.g., Benn & Astrom 2018; Colgan et al. 2016; Schulson 2002; van der Veen 1998a,b). Here, we focus on the links between fracture initiation and propagation to calving in ice shelves.

6.2.1. Crevasse depth–based calving laws. The earliest attempt to estimate crevasse depths assumed surface crevasses penetrate to the depth at which the horizontal stress vanishes (Nye 1957). This relationship, called the Nye zero stress model, was generalized by Jezek (1984) to

apply to water-filled basal crevasses. Alternatively, linear elastic fracture mechanics (LEFM) has been used to estimate the depth of surface and bottom crevasses, assuming they penetrate to the depth at which the intensity of the stress singularity (i.e., the stress intensity factor) is equal to the material fracture toughness (Rist et al. 2002, Smith 1976, Weertman 1980). Thus, LEFM typically results in deeper penetration of crevasses; however, Weertman (1976) reconciled the two estimates and showed that when closely spaced crevasses are considered in LEFM, interaction between crevasses reduces the stress singularity and results in a propagation criteria identical to that of Nye (1957). This has led to the terminology where the Nye zero stress model is assumed to apply to closely spaced crevasses, whereas the deeper crevasse depths associated with LEFM apply to isolated crevasses (e.g., Clayton et al. 2022). More complicated stress and geometric situations can be simulated with LEFM using tabulated interpolation functions for stress intensity factors (Lai et al. 2020; Rist et al. 2002; van der Veen 1998a,b) or, preferably, by computing stress intensity factors numerically (Jimenez & Duddu 2018). For both isolated and closely spaced crevasses, studies comparing estimated or measured depths based on field or satellite observations to predicted crevasse depths have been limited and yielded mixed results (Enderlin & Bartholomaus 2019, Mottram & Benn 2009).

6.2.2. Application of crevasse depth laws to glaciers and ice shelves. A version of crevasse depth–based calving laws treats every column of ice independently and predicts the position of the ice front by assuming calving occurs when calculated crevasse depths penetrate the ice thickness (or some fraction thereof) and isolate portions of ice from the main body of the glacier (Benn et al. 2007). This type of crevasse depth model does not predict individual fractures or calving events but an abstraction of fields of crevasses and the macroscopic effect these have on the calving front position. Crevasse depth–based calving laws were first successfully applied in a shallow-shelf flowline setting (Nick et al. 2007, 2009, 2010) but initially required that water depth is added as a tuning knob to allow full-thickness penetration of crevasses. Full stress balance (i.e., full Stokes models) leads to deeper crevasse penetration in grounded glaciers due to bending stresses near the calving front, eliminating the need for water depth tuning (Benn et al. 2017, Ma & Bassis 2019, Ma et al. 2017, Todd et al. 2018). However, crevasses are rarely predicted to instantaneously penetrate the entire ice thickness in floating ice shelves and ice tongues, and crevasse depth models have been less successful in these applications, a point we return to in Section 7.

6.3. Damage Mechanics

An alternative to fracture mechanics, damage mechanics relies on degrading the bulk material properties (e.g., the ice stiffness or viscosity) to assess or predict the collective weakening of glacier ice due to a distribution of cracks (Pralong & Funk 2005). The core idea of damage mechanics is that there is a mapping between the (true) Cauchy stress in a body with voids and cracks to an effective stress in a body devoid of any voids or defects. The effect of this mapping is typically to reduce the bulk material properties by a factor of (1-D), where D is a scalar damage variable that varies between 0 (intact) and 1 (fully broken). This scalar treatment of damage has been especially welcomed by the ice sheet modeling community because damage provides a systematic method to justify existing empirical adjustments to the stiffness of ice based on empirical evidence of material degradation (e.g., Borstad et al. 2012, 2013, 2017; Larour et al. 2021; Lhermitte et al. 2020). We focus here on scalar damage to simplify the exposition, but damage can be defined to be anisotropic, nonlocal, and generalized to include the effect of damage on permeability to describe hydrofracture. A related approach is the so-called phase-field fracture model, which treats damage as a distinct phase of matter with evolution of the material state determined by the minimization of free energy (Clayton et al. 2022, Sondershaus et al. 2023, Sun et al. 2021).

6.3.1. Creep-based damage production and crevasse depths.

The earliest attempts to integrate damage into glacier models translated a microscopic creep-damage formulation that uses a power-law damage evolution equation (e.g., Clayton et al. 2022; Duddu & Waisman 2012; Duddu et al. 2013, 2020; Mobasher et al. 2016; Pralong & Funk 2005; Pralong et al. 2003). The evolution equation for creep damage is stress based and formulated in terms of the Hayhurst criterion, a linear combination of the largest principal stress, the von Mises stress, and pressure (e.g., Pralong et al. 2003). In theory, the Hayhurst criterion can accommodate mixed-mode failure, but most simulations to date have focused on tensile failure. Moreover, with five tunable parameters and a paucity of data to constrain these parameters, modelers have great leeway to tune models to match laboratory or field observations. Despite the limitations, creep-based damage mechanics can naturally handle complicated geometries and boundary conditions and have been successful in reproducing surface and bottom crevasse depths predicted by LEFM and Nye zero models in idealized scenarios (e.g., Duddu et al. 2020).

6.3.2. Shallow-shelf implementation of damage mechanics.

At a higher level of approximation, but with a lower computational burden, creep damage has been integrated into shallow-shelf approximation and, with an appropriate initialization, shows promise in simulating the propagation of rifts in idealized and real ice shelves (Huth et al. 2021, 2023). A key feature of the creep-damage model is that the time-dependent production of damage is related to stress that phenomenologically represents localized failure processes in ice; the large-scale flow of the ice shelf, which adjusts more slowly, plays little role in driving creep damage. By contrast, Albrecht & Levermann (2012) proposed a phenomenological damage production function that depends on the largest principal strain rate.

6.3.3. Crevasse depth–based damage models.

An alternative approach that harkens back to the crevasse models (Section 6.2.1) defines the ratio of crevasse depth to ice thickness as a pseudo damage variable. For example, Sun et al. (2017) advect crevasse depths initiated with the Nye zero stress and consider the positive feedback between ice rheology and crevasse damage. By contrast, Bassis & Ma (2015) derived an evolution equation for the ratio of crevasse depth to ice thickness based on a linear-stability analysis in which crevasses, seeded by the Nye zero stress model, can evolve based on a necking instability and the difference in melt inside and outside of crevasses. This analytically deduced evolution law depends on strain rate, providing a physical basis for the phenomenological strain rate–based evolution law proposed by Albrecht & Levermann (2012), and provides a crucial connection between damage evolution and environmental forcing capable of explaining the lengths of contemporary observations of ice tongues and ice shelves (Kachuck et al. 2022).

6.4. Iceberg Resolving Models

At the highest level of complexity, models seek to resolve the processes involved in the formation and detachment of individual icebergs. For example, discrete element models (DEMs) represent glacier ice as a bonded assemblage of discrete boulders of ice. The DEM was first introduced by Cundall & Strack (1980) to represent the heterogenous brittle failure of rock assemblages and has been widely used to study brittle failure across a range of spatial and temporal scales. Early attempts to apply DEMs to glaciological situations showed that these methods can reproduce idealized patterns of calving (Astrom et al. 2013, Bassis & Jacobs 2013). The Helsinki Discrete Element Model (HiDEM) provides one of the more sophisticated glaciological implementations (Astrom et al. 2013). HiDEM creates glacier domains by creating lattices of particles linked by elastic breakable beams where broken beams can coalesce into large-scale fractures that propagate across

the domain. HiDEM was used to reproduce lab-scale compressive ice block fracture in 0.1- to 1-m scales (Prasanna et al. 2022). These lab-scale simulations are promising because simulations of the compressive brittle failure in ice remain difficult. Over larger glacier length scales, DEMs have been used to simulate the detachment patterns of individual icebergs, observed calving styles and the mechanical impact of mélange on the calving front of glaciers (Benn et al. 2017, Robel 2017), and, with appropriate modifications, patterns of fracture and calving on Antarctic ice shelves (e.g., Astrom & Benn 2019, Benn et al. 2022). DEMs are computationally expensive, and simulations are limited to relatively short timescales (minutes to hours) and typically do not include the longer-term viscous creep of the ice.

6.5. Shear Failure and Ice Cliff Instability

Most of the research on ice fracture has focused on tensile failure of ice. However, ice also fails in compression through the formation and coalescence of wing cracks and comb cracks into faults (e.g., Schulson 2002). It is this potential for shear failure that is the basis for the ice cliff instability (Bassis & Walker 2012), but it could also occur when ice is smashed into bathymetric highs [pinning points (e.g., Benn et al. 2022)]. Under the modest confining stresses typical of the surface of glaciers and ice sheets, brittle failure requires that the strain rate must also exceed the brittle-ductile strain rate or ductile flow will diminish stresses concentrated near cracks. If the brittle-ductile strain is exceeded, then shear localization is often represented by a Coulomb type of failure law of the form $|\tau_y| = \tau_c + \mu N$, where τ_y is the compressive strength, τ_c is the cohesion, μ denotes the coefficient of friction, and N is the effective normal stress (Schulson 2002). The coefficient of friction is believed to be a material property, but the cohesion, τ_c, and brittle-ductile strain rate depend on the size of preexisting flaws (Schulson 2002). Large preexisting flaws result in lower cohesion and a lower brittle-ductile strain rate resulting in lower barriers to shear failure.

6.5.1. Criterion for cliff stability and shear failure.
Only a handful of studies have examined shear failure in glaciological conditions. Bassis & Walker (2012) hypothesized that shear localization occurs when faults connect surface and basal crevasses. Because the depth averaged shear stress increases with ice thickness, this suggests that shear failure becomes more likely for tall ice cliffs that tower over the ocean. Subsequent studies instead show that slumping and shear failure connect seracs or surface crevasses with the waterline (**Figure 4**) (Parizek et al. 2019). Buoyancy
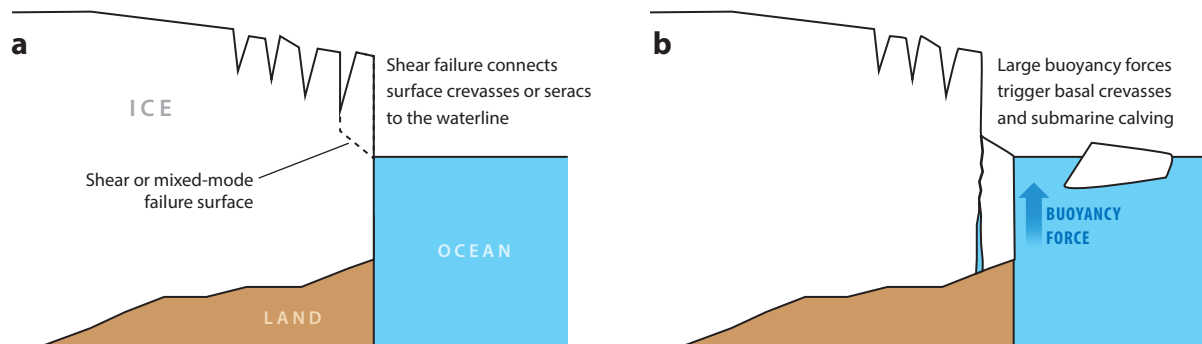
Figure 4

Schematic of a marine-terminating glacier illustrating faults and mixed-mode failure connecting surface crevasses or seracs to the waterline (*a*) followed by buoyancy-driven basal crevasse formation and propagation (*b*). Figure adapted from Parizek et al. (2019) and Trevers et al. (2019).

forces then trigger fractures that remove the submarine portion of the cliff (Bassis et al. 2021, Parizek et al. 2019). This process, illustrated in **Figure 4**, suggests that it is the height of the cliff above the waterline that controls structural stability. Carrying out a similar calculation to Bassis & Walker (2012) to estimate the depth averaged shear stress of the calving front that extends a height h above the surface of the water, the criterion for shear failure takes the form

$$h < \frac{4\tau_c}{\rho_i g}\frac{(1-r)}{(1-2\mu)}, \qquad 4.$$

where ρ_i is the density of ice, g is acceleration due to gravity, and r denotes the fraction of the cliff penetrated by surface crevasses and seracs. The above calculation ignores bending stresses near the front, resulting in an underestimation of the shear stress. Nonetheless, the primary uncertainty in determining the likelihood of shear failure is the cohesion τ_c, which is controlled by the size of preexisting flaws within the ice (Bassis et al. 2021, Clerc et al. 2019, Parizek et al. 2019). Clerc et al. (2019) argued that previous studies ignored visco-elastic relaxation and overestimated the conditions when shear failure is likely. The difference between predictions, however, lies in subtle assumptions about the strength of ice; the primary distinction in results is that Clerc et al. (2019) assumed preexisting flaw sizes are millimeters to centimeters in size (typical of laboratory settings) while Parizek et al. (2019) and Bassis et al. (2021) assumed starter flaws of the order of tens to hundreds of centimeters (typical of modern Greenland glaciers). At present, little is known about the size of preexisting flaws in ice. However, even when the size of flaws is known, the Coulomb failure criterion provides little guidance on rates at which failure occurs.

6.5.2. Models of shear localization and ice cliff failure.
Although DEMs have been effective in simulating brittle failure across a wide range of conditions, the restriction to brittle failure makes it more difficult to explore the balance between ductile flow and failure. Recent efforts, however, have shown promise in using fully viscous models to simulate the longer-term evolution of glaciers and then using HiDEM to resolve brittle fractures (Crawford et al. 2021). This iteration allows the interplay of long-term viscous creep and short-term brittle failure to be explored. An alternative approach that builds on methods commonly used in the geodynamics community seeks to simulate the failure of ice using plastic yield laws. For example, Bassis et al. (2021) examined flow and failure near the onset of the critical cliff height and demonstrated that ice cliff instability is governed by the balance between rates of brittle failure and the viscous thinning that reduces the cliff height. In this case, rapid dynamic ice thinning can stabilize or result in a quasi-stable retreat. However, this mechanism only works near the onset of failure. As the cliff height increases, modeling shows that the stresses and hence calving rates increase rapidly (Crawford et al. 2021). All these simulations are sensitive to the assumed distribution of preexisting flaws within the ice, and early work in this field has yet to fully examine the role of three-dimensional topography on failure and stability.

## 7. ICE SHELF STABILITY AND CLIMATE FORCING REVISITED

Despite the increasing sophistication of models of the calving process combined with the growing catalog of observations documenting ice shelf change, significant disagreement remains about the array of underlying processes driving calving. This is partly because models have often focused (or been tuned) to reproduce observations in particular glaciers, conditions, or environments. Moreover, there is a dizzying array of conflicting and seemingly contradictory observational studies in different environments that point at different controls on calving, which make it hard to decipher the overarching controls on ice shelf and marine glacier stability. For example, studies hint that the stability of some ice shelves is related to a compressive arch (Doake et al. 1998), but ice

tongues happily exist with no lateral confinement. Similarly, there is evidence that disintegration of ice shelves in some environments has been triggered by loss of sea ice, ocean swell, and other short-term environmental forcings, but other ice shelves show little sensitivity to short-term triggers. This diversity of environments and conditions eludes attempts to develop simple criteria to parameterize calving and poses significant challenges to models that need to represent all these different processes.

7.1. What Controls the Sensitivity of Ice Shelves to Long- and Short-Term Environmental Forcing?

Here we seek to reconcile these disparate results. As ice shelves thin—or once extensive fractures are present in the ice—stresses associated with ocean swell and other short-term environmental variables become an increasingly large component of the ice shelf stress balance. **Figure 5** shows the order of magnitude of stress associated with background gravitational stresses and a pulse of ocean swell. Thick ice shelves remain relatively insensitive to ocean swell, but as ice shelves thin [or become fractured (e.g., Lipovsky 2018)], they may become increasingly vulnerable to short-term environmental forcings present when sea ice and/or landfast ice is removed. This increasing sensitivity to environmental forces appears to be the dominant mode of ice shelf collapse in the Ellesmere Island Ice Shelves. This vulnerability, however, is preconditioned by the longer-term atmospheric and oceanic forcing that is ultimately responsible for thinning the ice shelves. Increased atmospheric temperatures can further destabilize ice shelves when conditions support the formation of melt ponds; surface meltwater is gravitationally unstable, and abundant meltwater trapped in depressions can trigger hydrofracture (e.g., Banwell & MacAyeal 2015, Banwell et al. 2013). All these studies hint that ice shelves are sometimes vulnerable to short-term environmental forcing (e.g., Wille et al. 2022), but this vulnerability needs to be preconditioned.
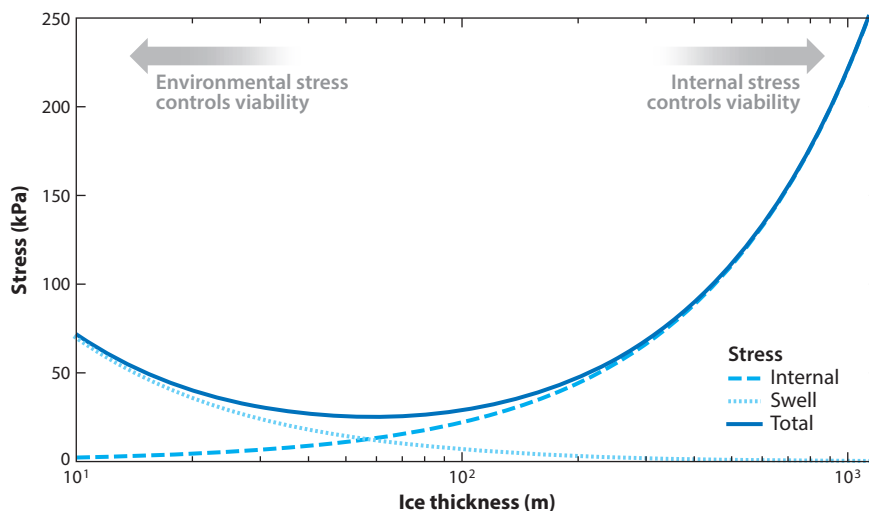
Figure 5

Estimate of forces driving calving that illustrate the role of long-term internal, glaciologic stress and shorter-term environmental stresses as a function of ice shelf thickness. For thin ice shelves, a 30-cm amplitude swell can provide a significant portion of the stress that the ice shelf experiences (*dotted line*). The contribution of environmental stress decreases for thick ice shelves, while the contribution by gravitationally driven internal stress increases (*dashed line*).

7.2. Glaciological Controls on Calving and Fracture Limited Stability

The thicker confined ice shelves common around the Antarctic Ice Sheet are less sensitive to shorter-term environmental conditions than many of the thinner ice shelves seen in Greenland and the Arctic. Many of these ice shelves are stabilized by lateral drag and constrained behind pinning points resulting in a compressive arch that prevents fractures from propagating across the center of the ice shelf. Pinning points and protrusions along the margins result in stress concentrations that serve as the initiation point of crevasses and, ultimately, rifting. As fractures advect beyond the embayment and into regions without confining stresses, conditions may allow large preexisting rifts to propagate laterally across large sections of the ice shelf and isolate large tabular bergs, perhaps analogous to the process modeled by Lipovsky (2020). However, this process is ultimately controlled by the production and advection of fractures that initiate in upstream regions. Unconfined ice tongues have little confining stresses, but the absence of margins and pinning points also results in fewer locations with a stress sufficient to seed fractures. Margins and pinning points of embayed ice shelves may play the dual role of stabilizing the ice shelves but also seeding the fractures that ultimately destabilize the ice shelf and become the detachment boundaries of icebergs.

7.3. Attractors and Stable Patterns of Calving

Given the disparity between observations of ice shelf and glacier change along with the limitations of modeling approaches, we revisit the concept of stability from a dynamical systems perspective. We hypothesize that stable patterns of calving front dynamics correspond to attractors in phase space. So long as the calving front fluctuates within the basin of attraction, patterns remain stable. The question is, how do we identify these attractors and the glaciological and environmental factors that control them? This remains an active area of research. However, there is a broad family of interrelated modeling approaches, including the Nye zero stress crevasse depth models (Benn et al. 2007), LEFM-based predictions of crevasse depth (Lai et al. 2020), the necking instability introduced by Bassis & Ma (2015), and the compressive arch proposed by Doake et al. (1998), that all provide similar answers. For example, denoting the ratio of depth averaged compressive to depth averaged tensile stresses by S_0, necking occurs when this dimensionless number is less than unity. Large values of S_0 correspond to the compressive arch of Doake et al. (1998), the inverse of S_0 is just the crevasse penetration ratio from the Nye zero stress model, and LEFM-based fracture depths can be expressed as a function of the same nondimensional parameter (Lai et al. 2020). All these different approaches ultimately provide a family of related approaches to determine the minimal extent of ice shelves and glaciers. This family of techniques, however, is built on the explicit assumption of tensile failure and cannot represent shear or mixed-mode failure associated with processes such as ice cliff instability.

7.4. Testing Models of Shear Failure and Ice Cliff Instability

Significant progress has been made in identifying and modeling key ice shelf processes, including fracture and failure. Theories of iceberg calving, ice shelf demise, and ice cliff instability must now be fully tested against a wide range of environmental and glaciological conditions in both modern and paleo conditions. This is especially true for the MICI, which has yet to be directly observed. Modern observations of thick Greenland and Antarctic glaciers provide some constraints on models, but the patchwork of paleo observations provides additional clues, constraints, and hints about the fundamental processes at work now and in the past. Even with these constraints, the theoretical foundation of ice cliff instability hinges on characterizing the difficult-to-measure

size of preexisting flaws, which may vary spatially and/or in time. Nonetheless, the presence of meter-scale flaws assumed in studies of ice shelf fracture (e.g., Lai et al. 2020, Rist et al. 2002) results in predicted cohesive strengths that are low enough that shear failure and faulting could occur in modern ice shelves when ice shelves are pushed into bedrock protrusions, providing a potentially rich testing ground to see when failure does and does not occur. In fact, studies have already identified faults and mixed-mode failure regimes in the Brunt and Thwaites ice shelves when the ice shelves collide with bedrock highs (Benn et al. 2022, Larour et al. 2014) and in a Greenlandic marine-terminating glacier (Hubbard et al. 2021). It is possible that mixed-mode fracture and faulting may be far more common in the fracture patterns that we currently observe, and this can be used to help constrain models of ice cliff failure.

7.5. Marine Ice Cliff Versus Marine Ice Sheet Instability

Currently, the MICI remains controversial and is viewed as a phenomenon that is distinct from the older and more established marine ice sheet instability. As we gather more observations and our understanding progresses, the distinction between ice sheet and ice cliff instability may ultimately be more nuanced. Large stresses are going to be created if thick grounding lines are exposed, and the distinction between MICI and marine ice sheet instability is largely a question of whether deformation is dominated by creep or failure; the reality is that it is likely that creep and fracture both have roles. An integrated view of marine ice cliff and marine ice sheet instability is needed to fully integrate the paleorecord into our understanding of the stability of marine-based ice sheets.

8. OPPORTUNITIES FOR ADVANCING OUR KNOWLEDGE OF ICE SHELF STABILITY

Atmospheric and ocean forcings are likely to continue to aggravate ice shelves, resulting in thinner and more fragile ice shelves that become increasingly vulnerable to environmental triggers. Continued ice shelf retreat may reveal new regimes and patterns of failure that we have yet to identify. To date, there is limited evidence that our current generation of models can predict ice shelf collapse or disintegration before it happens. The embarrassing reality is that, despite the increase in sophistication of our simulation toolsets, models have rarely successfully predicted major ice shelf or glacier changes before they occurred. Models have instead been used as forensic tools to hunt for clues about the causes and drivers of ice shelf change after they occur. However, with satellite observations with increasing temporal and spatial resolution, we find ourselves on the precipice of being able to observe fracture initiation and propagation with the potential to unearth new opportunities to study calving in near-real time. These new observations of ice shelf change provide opportunities to test and refine our understanding of key processes so that we move beyond our current forensic approach where we retroactively identify the taphonomy—or death assemblage of ice shelves—and instead formulate falsifiable hypotheses.

Advances in satellite data are providing insights into ice shelf changes in unprecedented detail. As we approach weekly or subweekly velocity coverage and meter-scale elevation, we can begin to resolve the details of fracture propagation at spatial and temporal resolutions that can calibrate, validate, and test existing theories of the calving processes at the fundamental scale. Constraining the stability of ice shelves, inherently dynamic and transient systems, requires unification of conceptual and quantitative frameworks across the many disparate fields of glaciology, paleoclimatology, materials science, and engineering. This integration that merges remote sensing, modeling, and paleo studies has the potential to provide better constraints in the paramount challenge of understanding projecting the past, present, and future behavior of ice shelves.

DISCLOSURE STATEMENT

ACKNOWLEDGMENTS

LITERATURE CITED

Albrecht T, Levermann A. 2012. Fracture field for large-scale ice dynamics. *J. Glaciol.* 58:165–76

Albrecht T, Levermann A. 2014. Spontaneous ice-front retreat caused by disintegration of adjacent ice shelf in Antarctica. *Earth Planet. Sci. Lett.* 393:26–30

Albrecht T, Martin M, Haseloff M, Winkelmann R, Levermann A. 2011. Parameterization for subgrid-scale motion of ice-shelf calving fronts. *Cryosphere* 5:35–44

Alley KE, Scambos TA, Siegfried MR, Fricker HA. 2016. Impacts of warm water on Antarctic ice shelf stability through basal channel formation. *Nat. Geosci.* 9:290–93

Alley KE, Wild CT, Luckman A, Scambos TA, Truffer M, et al. 2021. Two decades of dynamic change and progressive destabilization on the Thwaites Eastern Ice Shelf. *Cryosphere* 15:5187–203

Alley RB, Cuffey KM, Bassis JN, Alley KE, Wang S, et al. 2023. Iceberg calving: regimes and transitions. *Annu. Rev. Earth Planet. Sci.* 51:189–215

Alley RB, Horgan HJ, Joughin I, Cuffey KM, Dupont TK, et al. 2008. A simple law for ice-shelf calving. *Science* 322:1344

Aster RC, Lipovsky BP, Cole HM, Bromirski PD, Gerstoft P, et al. 2021. Swell-triggered seismicity at the near-front damage zone of the Ross Ice Shelf. *Seismol. Res. Lett.* 92:2768–92

Astrom JA, Benn DI. 2019. Effective rheology across the fragmentation transition for sea ice and ice shelves. *Geophys. Res. Lett.* 46:13099–106

Astrom JA, Riikila TI, Tallinen T, Zwinger T, Benn D, et al. 2013. A particle based simulation model for glacier dynamics. *Cryosphere* 7:1591–602

Banwell AF, Caballero M, Arnold NS, Glasser NF, Cathles LM, MacAyeal DR. 2014. Supraglacial lakes on the Larsen B ice shelf, Antarctica, and at Paakitsoq, West Greenland: a comparative study. *Ann. Glaciol.* 55:1–8

Banwell AF, MacAyeal DR. 2015. Ice-shelf fracture due to viscoelastic flexure stress induced by fill/drain cycles of supraglacial lakes. *Antarct. Sci.* 27:587–97

Banwell AF, MacAyeal DR, Sergienko OV. 2013. Breakup of the Larsen B Ice Shelf triggered by chain reaction drainage of supraglacial lakes. *Geophys. Res. Lett.* 40:5872–76

Bart PJ, Kratochvil M. 2022. A paleo-perspective on West Antarctic Ice Sheet retreat. *Sci. Rep.* 12:17693

Bassis JN. 2011. The statistical physics of iceberg calving and the emergence of universal calving laws. *J. Glaciol.* 57:3–16

Bassis JN, Berg B, Crawford AJ, Benn DI. 2021. Transition to marine ice cliff instability controlled by ice thickness gradients and velocity. *Science* 372:1342–44

Bassis JN, Fricker HA, Coleman R, Bock Y, Behrens J, et al. 2007. Seismicity and deformation associated with ice-shelf rift propagation. *J. Glaciol.* 53:523–36

Bassis JN, Fricker HA, Coleman R, Minster JB. 2008. An investigation into the forces that drive ice-shelf rift propagation on the Amery Ice Shelf, East Antarctica. *J. Glaciol.* 54:17–27

Bassis JN, Jacobs S. 2013. Diverse calving patterns linked to glacier geometry. *Nat. Geosci.* 6:833–36

Bassis JN, Ma Y. 2015. Evolution of basal crevasses links ice shelf stability to ocean forcing. *Earth Planet. Sci. Lett.* 409:203–11

Bassis JN, Walker CC. 2012. Upper and lower limits on the stability of calving glaciers from the yield strength envelope of ice. *Proc. R. Soc. A* 468:913–31

Batchelor CL, Christie FDW, Ottesen D, Montelli A, Evans J, et al. 2023. Rapid, buoyancy-driven ice-sheet retreat of hundreds of metres per day. *Nature* 617:105–10

Bell RE, Chu WN, Kingslake J, Das I, Tedesco M, et al. 2017. Antarctic ice shelf potentially stabilized by export of meltwater in surface river. *Nature* 544:344–48

Benn DI, Astrom J, Zwinger T, Todd J, Nick FM, et al. 2017. Melt-under-cutting and buoyancy-driven calving from tidewater glaciers: new insights from discrete element and continuum model simulations. *J. Glaciol.* 63:691–702

Benn DI, Astrom JA. 2018. Calving glaciers and ice shelves. *Adv. Phys. X* 3:1513819

Benn DI, Luckman A, Åström JA, Crawford AJ, Cornford SL, et al. 2022. Rapid fragmentation of Thwaites Eastern Ice Shelf. *Cryosphere* 16:2545–64

Benn DI, Warren CR, Mottram RH. 2007. Calving processes and the dynamics of calving glaciers. *Earth-Sci. Rev.* 82:143–79

Borstad C, McGrath D, Pope A. 2017. Fracture propagation and stability of ice shelves governed by ice shelf heterogeneity. *Geophys. Res. Lett.* 44:4186–94

Borstad CP, Khazendar A, Larour E, Morlighem M, Rignot E, et al. 2012. A damage mechanics assessment of the Larsen B ice shelf prior to collapse: toward a physically-based calving law. *Geophys. Res. Lett.* 39:L18502

Borstad CP, Rignot E, Mouginot J, Schodlok MP. 2013. Creep deformation and buttressing capacity of damaged ice shelves: theory and application to Larsen C ice shelf. *Cryosphere* 7:1931–47

Broberg KB. 1999. *Cracks and Fracture*. San Diego: Academic

Bromirski PD, Sergienko OV, MacAyeal DR. 2010. Transoceanic infragravity waves impacting Antarctic ice shelves. *Geophys. Res. Lett.* 37:L02502

Brunt KM, Okal EA, MacAyeal DR. 2011. Antarctic ice-shelf calving triggered by the Honshu (Japan) earthquake and tsunami, March 2011. *J. Glaciol.* 57:785–88

Campbell S, Courville Z, Sinclair S, Wilner J. 2017. Brine, englacial structure and basal properties near the terminus of McMurdo Ice Shelf, Antarctica. *Ann. Glaciol.* 58:1–11

Choi YM, Morlighem M, Wood M, Bondzio JH. 2018. Comparison of four calving laws to model Greenland outlet glaciers. *Cryosphere* 12:3735–46

Christianson K, Bushuk M, Dutrieux P, Parizek BR, Joughin IR, et al. 2016. Sensitivity of Pine Island Glacier to observed ocean forcing. *Geophys. Res. Lett.* 43:10817–25

Clayton T, Duddu R, Siegert M, Martinez-Paneda E. 2022. A stress-based poro-damage phase field model for hydrofracturing of creeping glaciers and ice shelves. *Eng. Fract. Mech.* 272:108693

Clerc F, Minchew BM, Behn MD. 2019. Marine ice cliff instability mitigated by slow removal of ice shelves. *Geophys. Res. Lett.* 46:12108–16

Colgan W, Rajaram H, Abdalati W, McCutchan C, Mottram R, et al. 2016. Glacier crevasses: observations, models, and mass balance implications. *Rev. Geophys.* 54:119–61

Copland L, Mortimer C, White A, McCallum MR, Mueller D. 2017. Factors contributing to recent Arctic ice shelf losses. In *Arctic Ice Shelves and Ice Islands*, ed. L Copland, D Mueller, pp. 263–85. Dordrecht, Neth.: Springer

Crawford AJ, Benn DI, Todd J, Astrom JA, Bassis JN, Zwinger T. 2021. Marine ice-cliff instability modeling shows mixed-mode ice-cliff failure and yields calving rate parameterization. *Nat. Commun.* 12:2701

Cundall PA, Strack ODL. 1980. A discrete numerical-model for granular assemblies—reply. *Geotechnique* 30:335–36

Davis PED, Jenkins A, Nicholls KW, Brennan PV, Abrahamsen EP, et al. 2018. Variability in basal melting beneath Pine Island Ice Shelf on weekly to monthly timescales. *J. Geophys. Res. Oceans* 123:8655–69

De Rydt J, Gudmundsson GH, Nagler T, Wuite J. 2019. Calving cycle of the Brunt Ice Shelf, Antarctica, driven by changes in ice shelf geometry. *Cryosphere* 13:2771–87

De Rydt J, Gudmundsson GH, Nagler T, Wuite J, King EC. 2018. Recent rift formation and impact on the structural integrity of the Brunt Ice Shelf, East Antarctica. *Cryosphere* 12:505–20

DeConto RM, Pollard D. 2016. Contribution of Antarctica to past and future sea-level rise. *Nature* 531:591–97

Doake CSM, Corr HFJ, Rott H, Skvarca P, Young NW. 1998. Breakup and conditions for stability of the northern Larsen Ice Shelf, Antarctica. *Nature* 391:778–80

Domack E, Duran D, Leventer A, Ishman S, Doane S, et al. 2005. Stability of the Larsen B ice shelf on the Antarctic Peninsula during the Holocene epoch. *Nature* 436:681–85

Dow CF, Lee WS, Greenbaum JS, Greene CA, Blankenship DD, et al. 2018. Basal channels drive active surface hydrology and transverse ice shelf fracture. *Sci. Adv.* 4:eaao7212

Dowdeswell JA. 2017. Eurasian Arctic ice shelves and tidewater ice margins. In *Arctic Ice Shelves and Ice Islands*, ed. L Copland, D Mueller, pp. 55–74. Dordrecht, Neth.: Springer

Dowdeswell JA, Gorman MR, Glazovsky AF, Macheret YY. 1994. Evidence for floating ice shelves in Franz-Josef-Land, Russian High Arctic. *Arctic Alpine Res.* 26:86–92

Duddu R, Bassis JN, Waisman H. 2013. A numerical investigation of surface crevasse propagation in glaciers using nonlocal continuum damage mechanics. *Geophys. Res. Lett.* 40:3064–68

Duddu R, Jimenez S, Bassis J. 2020. A non-local continuum poro-damage mechanics model for hydrofracturing of surface crevasses in grounded glaciers. *J. Glaciol.* 66:415–29

Duddu R, Waisman H. 2012. A temperature dependent creep damage model for polycrystalline ice. *Mech. Mater.* 46:23–41

Dutrieux P, Vaughan DG, Corr HFJ, Jenkins A, Holland PR, et al. 2013. Pine Island glacier ice shelf melt distributed at kilometre scales. *Cryosphere* 7:1543–55

Echelmeyer K, Clarke TS, Harrison WD. 1991. Surficial glaciology of Jakobshavns Isbrae, West Greenland: part 1. Surface-morphology. *J. Glaciol.* 37:368–82

Edwards TL, Brandon MA, Durand G, Edwards NR, Golledge NR, et al. 2019. Revisiting Antarctic ice loss due to marine ice-cliff instability. *Nature* 566:58–64

Enderlin EM, Bartholomaus TC. 2019. Poor performance of a common crevasse model at marine-terminating glaciers. *Cryosphere Discuss.* 2019:1–19

England J. 1999. Coalescent Greenland and Innuitian ice during the Last Glacial Maximum: revising the Quaternary of the Canadian High Arctic. *Quat. Sci. Rev.* 18:421–56

England JH, Evans DJA, Lakeman TR. 2017. Holocene history of Arctic ice shelves. In *Arctic Ice Shelves and Ice Islands*, ed. L Copland, D Mueller, pp. 185–205. Dordrecht, Neth.: Springer

England JH, Lakeman TR, Lemmen DS, Bednarski JM, Stewart TG, Evans DJA. 2008. A millennial-scale record of Arctic Ocean sea ice variability and the demise of the Ellesmere Island ice shelves. *Geophys. Res. Lett.* 35:L19502

Fox-Kemper B, Hewitt HT, Xiao C, Aðalgeirsdóttir G, Drijfhout SS, et al. 2021. Ocean, cryosphere and sea level change. In *Climate Change 2021: The Physical Science Basis. Contribution of Working Group I to the Sixth Assessment Report of the Intergovernmental Panel on Climate Change*, ed. V Masson-Delmotte, P Zhai, A Pirani, SL Connors, C Péan, et al., pp. 1211–362. Cambridge, UK: Cambridge Univ. Press

Francis D, Fonseca R, Mattingly KS, Marsh OJ, Lhermitte S, Cherif C. 2022. Atmospheric triggers of the brunt ice shelf calving in February 2021. *J. Geophys. Res. Atmos.* 127:e2021JD036424

Francis D, Mattingly KS, Lhermitte S, Temimi M, Heil P. 2021. Atmospheric extremes caused high oceanward sea surface slope triggering the biggest calving event in more than 50 years at the Amery Ice Shelf. *Cryosphere* 15:2147–65

Fricker HA, Young NW, Allison I, Coleman R. 2002. Iceberg calving from the Amery Ice Shelf, East Antarctica. *Ann. Glaciol.* 34(34):241–46

Glendinning P. 1994. *Stability, Instability, and Chaos: An Introduction to the Theory of Nonlinear Differential Equations*. New York: Cambridge Univ. Press

Goldberg D, Holland DM, Schoof C. 2009. Grounding line movement and ice shelf buttressing in marine ice sheets. *J. Geophys. Res.* 114(F4):F04026

Gomez-Fell R, Rack W, Purdie H, Marsh O. 2022. Parker Ice Tongue collapse, Antarctica, triggered by loss of stabilizing land-fast sea ice. *Geophys. Res. Lett.* 49:e2021GL096156

Graham AGC, Wåhlin A, Hogan KA, Nitsche FO, Heywood KJ, et al. 2022. Rapid retreat of Thwaites Glacier in the pre-satellite era. *Nat. Geosci.* 15:706–13

Grosswald MG, Hughes TJ. 2002. The Russian component of an Arctic Ice Sheet during the Last Glacial Maximum. *Quat. Sci. Rev.* 21:121–46

Haran T, Bohlander J, Scambos TA, Painter T, Fahnestock M. 2018a. *MEaSUREs MODIS Mosaic of Greenland (MOG) 2005, 2010, and 2015 Image Maps*. Boulder, CO: NASA Natl. Snow and Ice Data Cent.

Haran T, Klinger M, Bohlander J, Fahnestock M, Painter T, Scambos T. 2018b. *MEaSUREs MODIS Mosaic of Antarctica 2013–2014 (MOA2014) Image Map, Version 1*. Boulder, CO: NASA Natl. Snow and Ice Data Cent.

Hindmarsh RCA. 2012. An observationally validated theory of viscous flow dynamics at the ice-shelf calving front. *J. Glaciol.* 58:375–87

Hoffman MJ, Perego M, Price SF, Lipscomb WH, Zhang T, et al. 2018. MPAS-Albany Land Ice (MALI): a variable-resolution ice sheet model for Earth system modeling using Voronoi grids. *Geosci. Model Dev.* 11:3747–80

Holdsworth G, Glynn J. 1978. Iceberg calving from floating glaciers by a vibrating mechanism. *Nature* 274:464–66

Holland DM, Thomas RH, De Young B, Ribergaard MH, Lyberth B. 2008. Acceleration of Jakobshavn Isbrae triggered by warm subsurface ocean waters. *Nat. Geosci.* 1:659–64

Hoyle A. 2021. *Investigating North Greenland ice shelves and their response to warming climate*. PhD Diss., Scott Polar Res. Inst., Univ. Cambridge, Cambridge, UK

Hubbard B, Christoffersen P, Doyle SH, Chudley TR, Schoonman CM, et al. 2021. Borehole-based characterization of deep mixed-mode crevasses at a Greenlandic Outlet Glacier. *AGU Adv.* 2:e2020AV000291

Hughes T. 1977. West Antarctic ice streams. *Rev. Geophys.* 15:1–46

Hughes T, Denton GH, Grosswald MG. 1977. Was there a late-Würm Arctic ice sheet. *Nature* 266:596–602

Hulbe C, Fahnestock M. 2007. Century-scale discharge stagnation and reactivation of the Ross ice streams, West Antarctica. *J. Geophys. Res.* 112(F3):F03S27

Hulbe CL, LeDoux C, Cruikshank K. 2010. Propagation of long fractures in the Ronne Ice Shelf, Antarctica, investigated using a numerical model of fracture propagation. *J. Glaciol.* 56:459–72

Huth A, Duddu R, Smith B. 2021. A generalized interpolation material point method for shallow ice shelves. 2: Anisotropic nonlocal damage mechanics and rift propagation. *J. Adv. Model. Earth Syst.* 13:e2020MS002292

Huth A, Duddu R, Smith B, Sergienko O. 2023. Simulating the processes controlling ice-shelf rift paths using damage mechanics. *J. Glaciol.* 2023:1–14

Jakobsson M, Nilsson J, Anderson L, Backman J, Bjork G, et al. 2016. Evidence for an ice shelf covering the central Arctic Ocean during the penultimate glaciation. *Nat. Commun.* 7:10365

Jeffries MO. 1992. Arctic ice shelves and ice islands—origin, growth and disintegration, physical characteristics, structural-stratigraphic variability, and dynamics. *Rev. Geophys.* 30:245–67

Jeffries MO. 2017. The Ellesmere Ice Shelves, Nunavut, Canada. In *Arctic Ice Shelves and Ice Islands*, ed. L Copland, D Mueller, pp. 23–54. Dordrecht, Neth.: Springer

Jenkins A. 1991. A one-dimensional model of ice shelf-ocean interaction. *J. Geophys. Res.* 96(C11):20671–77

Jeong S, Howat IM, Bassis JN. 2016. Accelerated ice shelf rifting and retreat at Pine Island Glacier, West Antarctica. *Geophys. Res. Lett.* 43:11720–25

Jezek KC. 1984. Recent changes in the dynamic condition of the Ross Ice Shelf, Antarctica. *J. Geophys. Res.* 89(B1):409–16

Jimenez S, Duddu R. 2018. On the evaluation of the stress intensity factor in calving models using linear elastic fracture mechanics. *J. Glaciol.* 64:759–70

Joughin I, Abdalati W, Fahnestock M. 2004. Large fluctuations in speed on Greenland's Jakobshavn Isbrae glacier. *Nature* 432:608–10

Joughin I, MacAyeal DR. 2005. Calving of large tabular icebergs from ice shelf rift systems. *Geophys. Res. Lett.* 32:L02501

Joughin I, Shapero D, Smith B, Dutrieux P, Barham M. 2021. Ice-shelf retreat drives recent Pine Island Glacier speedup. *Sci. Adv.* 7:eabg3080

Kachuck SB, Whitcomb M, Bassis JN, Martin DF, Price SF. 2022. Simulating ice-shelf extent using damage mechanics. *J. Glaciol.* 68:987–98

Kilfeather AA, Cofaigh CO, Lloyd JM, Dowdeswell JA, Xu S, Moreton SG. 2011. Ice-stream retreat and ice-shelf history in Marguerite Trough, Antarctic Peninsula: sedimentological and foraminiferal signatures. *Geol. Soc. Am. Bull.* 123:997–1015

Kingslake J, Ely JC, Das I, Bell RE. 2017. Widespread movement of meltwater onto and across Antarctic ice shelves. *Nature* 544:349–52

Kulessa B, Jansen D, Luckman AJ, King EC, Sammonds PR. 2014. Marine ice regulates the future stability of a large Antarctic ice shelf. *Nat. Commun.* 5:3707

Lai CY, Kingslake J, Wearing MG, Chen PHC, Gentine P, et al. 2020. Vulnerability of Antarctica's ice shelves to meltwater-driven fracture. *Nature* 584:574–78

Larour E, Khazendar A, Borstad CP, Seroussi H, Morlighem M, Rignot E. 2014. Representation of sharp rifts and faults mechanics in modeling ice shelf flow dynamics: application to Brunt/Stancomb-Wills Ice Shelf, Antarctica. *J. Geophys. Res. Earth Surf.* 119:1918–35

Larour E, Rignot E, Poinelli M, Scheuchl B. 2021. Physical processes controlling the rifting of Larsen C Ice Shelf, Antarctica, prior to the calving of iceberg A68. *PNAS* 118:e2105080118

Lawn BR. 1993. *Fracture of Brittle Solids.* New York: Cambridge Univ. Press

Lazzara MA, Jezek KC, Scambos TA, MacAyeal DR, Van der Veen CJ. 2008. On the recent calving of icebergs from the Ross ice shelf. *Polar Geogr.* 31:15–26

Levermann A, Albrecht T, Winkelmann R, Martin MA, Haseloff M, Joughin I. 2012. Kinematic first-order calving law implies potential for abrupt ice-shelf retreat. *Cryosphere* 6:273–86

Lhermitte S, Sun SN, Shuman C, Wouters B, Pattyn F, et al. 2020. Damage accelerates ice shelf instability and mass loss in Amundsen Sea Embayment. *PNAS* 117:24735–41

Lipovsky BP. 2018. Ice shelf rift propagation and the mechanics of wave-induced fracture. *J. Geophys. Res. Oceans* 123:4014–33

Lipovsky BP. 2020. Ice shelf rift propagation: stability, three-dimensional effects, and the role of marginal weakening. *Cryosphere* 14:1673–83

Lipscomb WH, Price SF, Hoffman MJ, Leguy GR, Bennett AR, et al. 2019. Description and evaluation of the Community Ice Sheet Model (CISM) v2.1. *Geosci. Model Dev.* 12:387–424

Liu Y, Moore JC, Cheng X, Gladstone RM, Bassis JN, et al. 2015. Ocean-driven thinning enhances iceberg calving and retreat of Antarctic ice shelves. *PNAS* 112:3263–68

Ma Y, Bassis JN. 2019. The effect of submarine melting on calving from marine terminating glaciers. *J. Geophys. Res. Earth Surf.* 124:334–46

Ma Y, Tripathy CS, Bassis JN. 2017. Bounds on the calving cliff height of marine terminating glaciers. *Geophys. Res. Lett.* 44:1369–75

MacAyeal DR, Scambos TA, Hulbe CL, Fahnestock MA. 2003. Catastrophic ice-shelf break-up by an ice-shelf-fragment-capsize mechanism. *J. Glaciol.* 49:22–36

Majewski W, Bart PJ, McGlannan AJ. 2018. Foraminiferal assemblages from ice-proximal paleo-settings in the Whales Deep Basin, eastern Ross Sea, Antarctica. *Palaeogeogr. Palaeoclimatol. Palaeoecol.* 493:64–81

Massom RA, Giles AB, Fricker HA, Warner RC, Legresy B, et al. 2010. Examining the interaction between multi-year landfast sea ice and the Mertz Glacier Tongue, East Antarctica: another factor in ice sheet stability? *J. Geophys. Res.* 115(C12):C12027

Massom RA, Giles AB, Warner RC, Fricker HA, Legresy B, et al. 2015. External influences on the Mertz Glacier Tongue (East Antarctica) in the decade leading up to its calving in 2010. *J. Geophys. Res. Earth Surf.* 120:490–506

Massom RA, Scambos TA, Bennetts LG, Reid P, Squire VA, Stammerjohn SE. 2018. Antarctic ice shelf disintegration triggered by sea ice loss and ocean swell. *Nature* 558:383–89

Mercer JH. 1970. A former ice sheet in the Arctic Ocean? *Palaeogeogr. Palaeoclimatol. Palaeoecol.* 8:19–27

Mercer JH. 1978. West Antarctic ice sheet and CO_2 greenhouse effect: a threat of disaster. *Nature* 271:321–25

Miles BWJ, Stokes CR, Jamieson SSR. 2017. Simultaneous disintegration of outlet glaciers in Porpoise Bay (Wilkes Land), East Antarctica, driven by sea ice break-up. *Cryosphere* 11:427–42

Miles BWJ, Stokes CR, Jamieson SSR. 2018. Velocity increases at Cook Glacier, East Antarctica, linked to ice shelf loss and a subglacial flood event. *Cryosphere* 12:3123–36

Miles BWJ, Stokes CR, Jenkins A, Jordan JR, Jamieson SSR, Gudmundsson GH. 2020. Intermittent structural weakening and acceleration of the Thwaites Glacier Tongue between 2000 and 2018. *J. Glaciol.* 66:485–95

Milillo P, Rignot E, Rizzoli P, Scheuchl B, Mouginot J, et al. 2019. Heterogeneous retreat and ice melt of Thwaites Glacier, West Antarctica. *Sci. Adv*. 5:eaau3433

Mobasher ME, Duddu R, Bassis JN, Waisman H. 2016. Modeling hydraulic fracture of glaciers using continuum damage mechanics. *J. Glaciol*. 62:794–804

Moon T, Joughin I. 2008. Changes in ice front position on Greenland's outlet glaciers from 1992 to 2007. *J. Geophys. Res*. 113(F3):F02022

Morlighem M, Bondzio J, Seroussi H, Rignot E, Larour E, et al. 2016. Modeling of Store Gletscher's calving dynamics, West Greenland, in response to ocean thermal forcing. *Geophys. Res. Lett*. 43:2659–66

Mottram RH, Benn DI. 2009. Testing crevasse-depth models: a field study at Breioamerkurjokull, Iceland. *J. Glaciol*. 55:746–52

Mueller D, Copland L, Jeffries MO. 2017a. Changes in Canadian Arctic ice shelf extent since 1906. In *Arctic Ice Shelves and Ice Islands*, ed. L Copeland, D Mueller, pp. 109–48. Dordrecht, Neth.: Springer

Mueller D, Copland L, Jeffries MO. 2017b. Northern Ellesmere Island ice shelf and ice tongue extents, v. 1.0 (1906–2015). *Nordicana D28* 2017:10

Munchow A, Padman L, Washam P, Nicholls KW. 2016. The ice shelf of Petermann Gletscher, North Greenland, and its connection to the Arctic and Atlantic Oceans. *Oceanography* 29:84–95

Needell C, Holschuh N. 2023. Evaluating the retreat, arrest, and regrowth of Crane Glacier against marine ice cliff process models. *Geophys. Res. Lett*. 50:e2022GL102400

Nick FM, van der Veen CJ, Oerlemans J. 2007. Controls on advance of tidewater glaciers: results from numerical modeling applied to Columbia Glacier. *J. Geophys. Res*. 112(F3):F03S24

Nick FM, van der Veen CJ, Vieli A, Benn DI. 2010. A physically based calving model applied to marine outlet glaciers and implications for the glacier dynamics. *J. Glaciol*. 56:781–94

Nick FM, Vieli A, Howat IM, Joughin I. 2009. Large-scale changes in Greenland outlet glacier dynamics triggered at the terminus. *Nat. Geosci*. 2:110–14

Nye JF. 1957. The distribution of stress and velocity in glaciers and ice-sheets. *Proc. R. Soc. A* 239:113–33

Olinger SD, Lipovsky BP, Wiens DA, Aster RC, Bromirski PD, et al. 2019. Tidal and thermal stresses drive seismicity along a major Ross Ice Shelf rift. *Geophys. Res. Lett*. 46:6644–52

Paolo FS, Fricker HA, Padman L. 2015. Volume loss from Antarctic ice shelves is accelerating. *Science* 348:327–31

Parizek BR, Christianson K, Alley RB, Voytenko D, Vankova I, et al. 2019. Ice-cliff failure via retrogressive slumping. *Geology* 47:449–52

Phillips HA. 1998. Surface meltstreams on the Amery Ice Shelf, East Antarctica. *Ann. Glaciol*. 27(27):177–81

Polyak L, Edwards MH, Coakley BJ, Jakobsson M. 2001. Ice shelves in the Pleistocene Arctic Ocean inferred from glaciogenic deep-sea bedforms. *Nature* 410:453–57

Pralong A, Funk M. 2005. Dynamic damage model of crevasse opening and application to glacier calving. *J. Geophys. Res*. 110(B1):B01309

Pralong A, Funk M, Luthi MP. 2003. A description of crevasse formation using continuum damage mechanics. *Ann. Glaciol*. 37(37):77–82

Prasanna M, Polojarvi A, Wei MD, Astrom J. 2022. Modeling ice block failure within drift ice and ice rubble. *Phys. Rev. E* 105:045001

Pritchard HD, Arthern RJ, Vaughan DG, Edwards LA. 2009. Extensive dynamic thinning on the margins of the Greenland and Antarctic ice sheets. *Nature* 461:971–75

Rack W, Rott H. 2004. Pattern of retreat and disintegration of the Larsen B ice shelf, Antarctic Peninsula. *Ann. Glaciol*. 39(39):505–10

Reeh N, Thomsen HH, Higgins AK, Weidick A. 2001. Sea ice and the stability of north and northeast Greenland floating glaciers. *Ann. Glaciol*. 33(33):474–80

Rist MA, Sammonds PR, Oerter H, Doake CSM. 2002. Fracture of Antarctic shelf ice. *J. Geophys. Res*. 107(B1):ECV 2-1–ECV 2-13

Robel AA. 2017. Thinning sea ice weakens buttressing force of iceberg melange and promotes calving. *Nat. Commun*. 8:14596

Rott H, Rack W, Nagler T, Skvarca P. 1998. Climatically induced retreat and collapse of northern Larsen Ice Shelf, Antarctic Peninsula. *Ann. Glaciol*. 27(27):86–92

Ruckamp M, Neckel N, Berger S, Humbert A, Helm V. 2019. Calving induced speedup of Petermann Glacier. *J. Geophys. Res. Earth Surf.* 124:216–28

Scambos T, Hulbe C, Fahnestock M. 2003. Climate-induced ice shelf disintegration in the Antarctic Peninsula. *Antarct. Penins. Clim. Var. Hist. Paleoenviron. Perspect.* 79:79–92

Scambos TA, Bell RE, Alley RB, Anandakrishnan S, Bromwich DH, et al. 2017. How much, how fast?: A science review and outlook for research on the instability of Antarctica's Thwaites Glacier in the 21st century. *Glob. Planet. Change* 153:16–34

Scambos TA, Bohlander JA, Shuman CA, Skvarca P. 2004. Glacier acceleration and thinning after ice shelf collapse in the Larsen B embayment, Antarctica. *Geophys. Res. Lett.* 31:L18402

Schmidt BE, Washam P, Davis PED, Nicholls KW, Holland DM, et al. 2023. Heterogeneous melting near the Thwaites Glacier grounding line. *Nature* 614:471–78

Schoof C. 2012. Marine ice sheet stability. *J. Fluid Mech.* 698:62–72

Schulson EM. 2002. Brittle failure of ice. *Plast. Deform. Minerals Rocks* 51:201–52

Skvarca P. 1993. Fast recession of the northern Larsen Ice Shelf monitored by space images. *Ann. Glaciol.* 17:317–21

Smith R. 1976. The application of fracture mechanics to the problem of crevasse penetration. *J. Glaciol.* 17:223–28

Sondershaus R, Humbert A, Müller R. 2023. A phase field model for fractures in ice shelves. *PAMM* 22:e202200256

Spergel JJ, Kingslake J, Creyts T, van Wessem M, Fricker HA. 2021. Surface meltwater drainage and ponding on Amery Ice Shelf, East Antarctica, 1973–2019. *J. Glaciol.* 67:985–98

Sun S, Cornford SL, Moore JC, Gladstone R, Zhao LY. 2017. Ice shelf fracture parameterization in an ice sheet model. *Cryosphere* 11:2543–54

Sun XM, Duddu R, Hirshikesh. 2021. A poro-damage phase field model for hydrofracturing of glacier crevasses. *Extreme Mech. Lett.* 45:101277

Thomas RH, MacAyeal DR. 1978. Glaciological measurements on the Ross Ice Shelf. *Antarct. J. U. S.* 13:55–56

Todd J, Christoffersen P, Zwinger T, Raback P, Chauche N, et al. 2018. A full-Stokes 3-D calving model applied to a large Greenlandic glacier. *J. Geophys. Res. Earth Surf.* 123:410–32

Trevers M, Payne AJ, Cornford SL, Moon T. 2019. Buoyant forces promote tidewater glacier iceberg calving through large basal stress concentrations. *Cryosphere* 13:1877–87

van der Veen CJ. 1996. Tidewater calving. *J. Glaciol.* 42:375–85

van der Veen CJ. 1998a. Fracture mechanics approach to penetration of bottom crevasses on glaciers. *Cold Regions Sci. Technol.* 27:213–23

van der Veen CJ. 1998b. Fracture mechanics approach to penetration of surface crevasses on glaciers. *Cold Regions Sci. Technol.* 27:31–47

van Wessem JM, van den Broeke MR, Wouters B, Lhermitte S. 2023. Variable temperature thresholds of melt pond formation on Antarctic ice shelves. *Nat. Clim. Change* 13:161–66

Vaughan DG, Corr HFJ, Bindschadler RA, Dutrieux P, Gudmundsson GH, et al. 2012. Subglacial melt channels and fracture in the floating part of Pine Island Glacier, Antarctica. *J. Geophys. Res.* 117(F3):F03012

Vaughan DG, Doake CSM. 1996. Recent atmospheric warming and retreat of ice shelves on the Antarctic Peninsula. *Nature* 379:328–31

Vermassen F, Bjork AA, Sicre MA, Jaeger JM, Wangner DJ, et al. 2020. A major collapse of Kangerlussuaq Glacier's ice tongue between 1932 and 1933 in East Greenland. *Geophys. Res. Lett.* 47:e2019GL085954

Vieli A, Nick FM. 2011. Understanding and modelling rapid dynamic changes of tidewater outlet glaciers: issues and implications. *Surveys Geophys.* 32:437–58

Vincent WF, Gibson JAE, Jeffries MO. 2001. Ice-shelf collapse, climate change, and habitat loss in the Canadian high Arctic. *Polar Record* 37:133–42

Vincent WF, Mueller D. 2020. Witnessing ice habitat collapse in the Arctic. *Science* 370:1031–32

Walker CC, Bassis JN, Fricker HA, Czerwinski RJ. 2013. Structural and environmental controls on Antarctic ice shelf rift propagation inferred from satellite monitoring. *J. Geophys. Res. Earth Surf.* 118:2354–64

Walker CC, Bassis JN, Fricker HA, Czerwinski RJ. 2015. Observations of interannual and spatial variability in rift propagation in the Amery Ice Shelf, Antarctica, 2002–14. *J. Glaciol.* 61:243–52

Walker CC, Becker MK, Fricker HA. 2021. A high resolution, three-dimensional view of the D-28 calving event from Amery Ice Shelf with ICESat-2 and satellite imagery. *Geophys. Res. Lett.* 48:e2020GL091200

Walter F, O'Neel S, McNamara D, Pfeffer WT, Bassis JN, Fricker HA. 2010. Iceberg calving during transition from grounded to floating ice: Columbia Glacier, Alaska. *Geophys. Res. Lett.* 37:L15501

Watkins RH, Bassis JN, Thouless MD. 2021. Roughness of ice shelves is correlated with basal melt rates. *Geophys. Res. Lett.* 48:e2021GL094743

Weertman J. 1974. Stability of the junction of an ice sheet and an ice shelf. *J. Glaciol.* 13:3–11

Weertman J. 1976. Penetration depth of closely spaced crevasses. *Trans.-Am. Geophys. Union* 57:324–25

Weertman J. 1980. Bottom crevasses. *J. Glaciol.* 25:185–88

White A, Copland L, Mueller D, Van Wychen W. 2015. Assessment of historical changes (1959–2012) and the causes of recent break-ups of the Petersen ice shelf, Nunavut, *Canada. Ann. Glaciol.* 56(69):65–76

Wille JD, Favier V, Jourdain NC, Kittel C, Turton JV, et al. 2022. Intense atmospheric rivers can weaken ice shelf stability at the Antarctic Peninsula. *Commun. Earth Environ.* 3:90

Williams M, Dowdeswell JA. 2001. Historical fluctuations of the Matusevich Ice Shelf, Severnaya Zemlya, Russian High Arctic. *Arctic Antarct. Alp. Res.* 33:211–22

Wise MG, Dowdeswell JA, Jakobsson M, Larter RD. 2017. Evidence of marine ice-cliff instability in Pine Island Bay from iceberg-keel plough marks. *Nature* 550:506–10

Yu HJ, Rignot E, Seroussi H, Morlighem M, Choi YM. 2019. Impact of iceberg calving on the retreat of Thwaites Glacier, West Antarctica over the next century with different calving laws and ocean thermal forcing. *Geophys. Res. Lett.* 46:14539–47